2002), their all-method-principle and all-instruments CVs ranged from ~4% to 7% (*10, 11*), similar to our findings. We chose to exclude results from two laboratories that reported a gelatinous material in the TIBC medium pool and chose not to impute values for one laboratory that did not report raw values for the UIBC low pool. Additionally, we excluded 13 values from the ~1650 analyte values; these, however, represent <1% of all values and should not reduce interpretation of analytic validity.

References

1. Powell LW, George DK, McDonnell SM, Kowdley KV. Diagnosis of hemochromatosis. Ann Intern Med 1998;129:925–31.
2. Giovaniello TJ, Bendetto G, Palmer DW, Peters T. Fully and semiautomated methods for the determination of serum iron and total iron-binding capacity. J Lab Clin Med 1968;71:874.
3. Gunter EW, Lewis BL, Koncikowski SM. Laboratory methods used for the Third National Health and Nutrition Examination Survey (NHANES III), 1988–1994. Hyattsville, MD: Centers for Disease Control and Prevention, 1997.
4. National Committee for Clinical Laboratory Standards. Determination of serum iron, total iron-binding capacity and percent transferrin saturation; approved standard. NCCLS document H17-A. Wayne, PA: NCCLS, 1998.
5. Witte DL, Crosby WH, Edwards CQ, Fairbanks VF, Mitros FA. Practice guideline development task force of the College of American Pathologists. Hereditary hemochromatosis. Clin Chim Acta 1996;245:139–200.
6. Dixon WJ. Processing data for outliers. Biometrics 1953;9:74–89.
7. SAS Institute Inc. SAS/STAT user's guide, Ver. 8. Cary, NC: SAS Institute Inc., 1999:3884pp.
8. Bartlett MS. Some applications of statistical methods of research in agriculture and applied biology. J R Stat Soc Suppl 1937;4:137–83.
9. Bland JM, Altman DG. Multiple significance tests: the Bonferroni method. BMJ 1995;310:170.
10. College of American Pathologists. Chemistry survey, set C-B 2001, participant summary. Northfield, IL: College of American Pathologists, 2001.
11. College of American Pathologists. Chemistry survey, set C-A 2002, participant summary. Northfield, IL: College of American Pathologists, 2002.

CARD15 Genotyping in Inflammatory Bowel Disease Patients by Multiplex Pyrosequencing,

Orazio Palmieri,[1,2] Stephen Toth,[3] Alessandro Ferraris,[4,5,6] Angelo Andriulli,[2] Anna Latiano,[2] Vito Annese,[2] Bruno Dallapiccola,[4,5,6] Maurizio Vecchi,[7] Marcella Devoto,[8,9] Saul Surrey,[1] and Paolo Fortina[1]* ([1] Department of Medicine, Thomas Jefferson University, Jefferson Medical College, Philadelphia, PA 19104; [2] Unita'di Ricerca in Gastroenterologia, IRCCS Casa Sollievo della Sofferenza, I-71013 San Giovanni Rotondo, Italy; [3] Pyrosequencing, Inc., Westborough, MA 01581; [4] IRCCS C.S.S., I-71013 San Giovanni Rotondo, Italy; [5] C.S.S.-Mendel, 00161 Rome, Italy; [6] Dipartimento di Medicina Sperimentale e Patologia, Universitá "La Sapienza", 00161 Rome, Italy; [7] Istituto e Servizio di Gastroenterologia, IRCCS Ospedale Maggiore e Universitá di Milano, 20122 Milan, Italy; [8] Department of Biomedical Research, Nemours Children's Clinic, Wilmington, DE 19880; [9] Dipartimento di Oncologia, Biologia e Genetica, Universitá di Genova, 16146 Genoa, Italy; * address correspondence to this author at: 406 Medical Office Bldg., 1100 Walnut St., Philadelphia, PA 19107; fax 215-955-6905, e-mail paolo.fortina@jefferson.edu)

We describe here a method for detection of three common single-nucleotide polymorphisms (SNPs) in the inflammatory bowel disease (IBD)-related *CARD15* gene. We used a two-step approach with multiplex PCR and pyrosequencing. Although the three loci are spaced far from one another, the built-in multiplexing capability of pyrosequencing reactions to extend for numerous bases was used with appropriate primers and the design of efficient deoxynucleoside triphosphate (dNTP) dispensation orders to screen for the variants simultaneously.

IBDs are chronic relapsing disorders affecting the gastrointestinal tract with a population prevalence in Western countries of 1:1000 (*1*). The complex trait is subdivided on the basis of clinical and histologic features into two main subtypes: Crohn disease (CD) and ulcerative colitis (UC) (*2–5*). Whereas UC is limited to the rectal and colonic mucosal layers, CD can involve any part of the intestine, most frequently the terminal ileum and colon (*6–9*). Several candidate loci for IBD have been identified on the basis of whole-genome scans in different populations (*10–18*). Of these, the one on chromosome 16 named *IBD1* has been confirmed in several independent studies (*11, 12, 15–18*). Three SNPs in the *CARD15* gene, located in the *IBD1* region, have been demonstrated to confer susceptibility to CD, but not to UC, in several populations and to correlate with an ileal site of the disease (*6–10*).

In this report, using a previously described approach for SNP/mutation analysis (*19*), we developed and validated a protocol to characterize simultaneously the R702W (SNP8), G908R (SNP12), and L1007fsinsC (SNP13) variants, which are associated with increased risk of CD (*20–22*). Although additional *CARD15* variants have been found to be associated to CD, these are the three most common and are found in almost all populations tested (*7*).

A total of 141, 163, and 61 individuals from 47 CD, 49

UC, and 18 mixed (containing affected members with both CD and UC) families, respectively, and 108 unrelated healthy controls were included in the study after informed consent. Genomic DNA samples were purified from peripheral blood leukocytes according to standard protocols or with the Puregene DNA isolation reagent set (Gentra System).

Multiplex PCR reactions were performed on samples to be genotyped for the three variants (R702W, G908R, and L1007fsinsC) in the *CARD15* gene. PCR and Pyrosequencing sequencing primers were designed according to Pyrosequencing guidelines (http://www.pyrosequencing. com). Briefly, three fragments of 106, 117, and 104 bp, respectively, encompassing the three SNPs were PCR-amplified using forward and the reverse primer pairs R702W-F (5'-TTC CTG GCA GGG CTG TT-3') and R702W-R (5'-biotin-CCA GAC ACC AGC GGG C-3'), G908R-F (5'-**T**AG AGG GAG GAG GAC TGT TAG TT-3') and G908R-R (5'-biotin-CCC CCT CGT CAC CCA CT-3'), and L1007fsinsC-F (5'-**T**CC TTA CCA GAC TTC CAG GAT G-3') and L1007fsinsC-R (5'-biotin-TCT TCT TTT CCA GGT TGT CCA-3') with one of the two PCR primers (Integrated DNA Technologies) for each SNP containing biotin at the 5'-terminus to facilitate isolation of a single-stranded template for the Pyrosequencing assay. All primers were HPLC-purified.

Because a template hairpin was predicted by SNP Primer Design software Ver. 1.0 (Pyrosequencing AB), a nonmatching T (underlined and bolded above) was added to the 5' end of the nonbiotinylated PCR primers for the G908R and L1007fsinsC SNPs to prevent extension from these templates. The triplex PCR reactions were done in a final volume of 50 μL containing GeneAmp 1$\times$ Buffer II (10 mM Tris-HCl, pH 8.3; 50 mM KCl), 2.5 mM MgCl$_2$, 3 U of AmpliTaq Gold DNA polymerase (Applied Biosystems), 200 nM each primer, 1 mM dNTPs (Amersham Pharmacia Biotech), and 50 ng of the genomic DNA. Reactions were performed with initial denaturation at 95 °C for 10 min, followed by 35 cycles at 95 °C for 1 min, annealing at 62 °C for 1 min, and extension at 72 °C for 1 min. Final extension was 72 °C for 10 min.

Bound biotinylated single-stranded DNA was generated using protocols recommended by the manufacturer (PSQ^{TM} HS 96A System Sample Preparation Kit; Pyrosequencing AB). The biotinylated triplex PCR products (5 μL) were bound to streptavidin-Sepharose HP beads (2 μL; Amersham Biosciences) and incubated with binding buffer pH 7.6 (38 μL; 10 mmol/L Tris-HCl, 2 mol/L NaCl, 1 mmol/L EDTA, 1 mL/L Tween 20) and diethylpyrocarbonate-treated water (30 μL; Ambion) in a 96-well microtiter plate for 15 min at 40 °C with mixing at 1400 rpm in a Thermomixer R (Eppendorf). The 96-well plate was subjected to vacuum filtration using the Vacuum Prep Tool (Pyrosequencing AB), which consists of a hand-grip with 96-filter probes. The bead-bound PCR products were transferred to the filter at the end of each 96-filter probe, and the remaining liquid was removed by vacuum filtration. The Vacuum Prep Tool was transferred to a trough containing 700 mL/L ethanol for 5 s. Nonbiotinylated strands were removed after treatment with denaturation solution (0.2 mol/L NaOH) for 5 s. Bead-bound biotinylated strands were retained on the filter and rinsed in washing buffer (10 mmol/L Tris-acetate, pH 7.6) for 7 s. The vacuum was removed to release beads from the filter. Bead-bound single-stranded DNA templates for each SNP were resuspended in annealing buffer (12 μL; 20 mM Tris-acetate, pH 7.6; 2 mM magnesium acetate) containing 0.5 μM (6 pmol) of the HPLC-purified Pyrosequencing primers R702W-F (5'-A CAT **TG**G AGA AGG CCC-3'), G908R-F (5'-CTT TT**A A**CC TTT TCA G-3'), and L1007fsinsC-F (5'-TGT CAT TCC TTT CAA GGG-3') in wells of a PSQ 96 plate (Pyrosequencing AB). To prevent extension from sequencing primers self-annealing, TG and AA mismatches (underlined and bolded above) were added to the R702W and G908R Pyrosequencing sequencing primers, respectively. Pyrosequencing assay design flexibility and chemistry made it possible to introduce these specific mismatches without affecting sequencing results. The mixture was heated at 94 °C for 2 min and then cooled to room temperature to facilitate annealing of the Pyrosequencing primers to templates. The plate was placed into the PSQ HS 96A System for analysis (Pyrosequencing AB).

An automated Pyrosequencing instrument, PSQ HS 96A (Pyrosequencing AB), was used to perform multiplex genotyping in a single Pyrosequencing reaction at 28 °C. Each well contained Sepharose beads with the bound single-stranded DNA template and its annealed Pyrosequencing primer. The Pyrosequencing reaction began with the addition of enzymes (DNA polymerase exonuclease-deficient, apyrase, luciferase, ATP sulfurylase) and substrates (adenosine 5'-phosphosulfate and luciferin) to each well. Individual dNTPs [TTP, dGTP, dCTP, or deoxyadenosine α-thio-triphosphate (dATPαS)] were sequentially added to the reactions after each elongation reaction step. Excess nucleoside triphosphates from the previous step were degraded by apyrase. Only one dNTP was added at each step according to a dispensation order (CGC TAT CGT GCG CTC TGA GA) entered in the Pyrosequencing SNP Multiplex Entry software (Pyrosequencing AB), which was selected to allow for simultaneous detection of all three SNPs. The sequence of incorporated nucleoside at each elongation step was inferred by measuring light emission as an indicator of incorporation with the particular dispensed dNTP. The resulting sequences were analyzed automatically by the SNP evaluation software, Ver. 1.1 (Pyrosequencing AB). Each SNP in all samples was confirmed by DNA sequence analysis with the ABI BigDye Terminator, Ver. 3.1, Cycle Sequencing Ready Reaction on a ABI 3100 DNA sequencer (Applied Biosystems) according to the manufacturer's recommendations.

Three different primers pairs were used for multiplex PCR, and three different Pyrosequencing primers were used for simultaneous detection of the three SNPs in the *CARD15* gene in a single Pyrosequencing reaction. For triplex *CARD15* SNP genotyping, a dispensation order was determined that allowed each SNP variant to appear
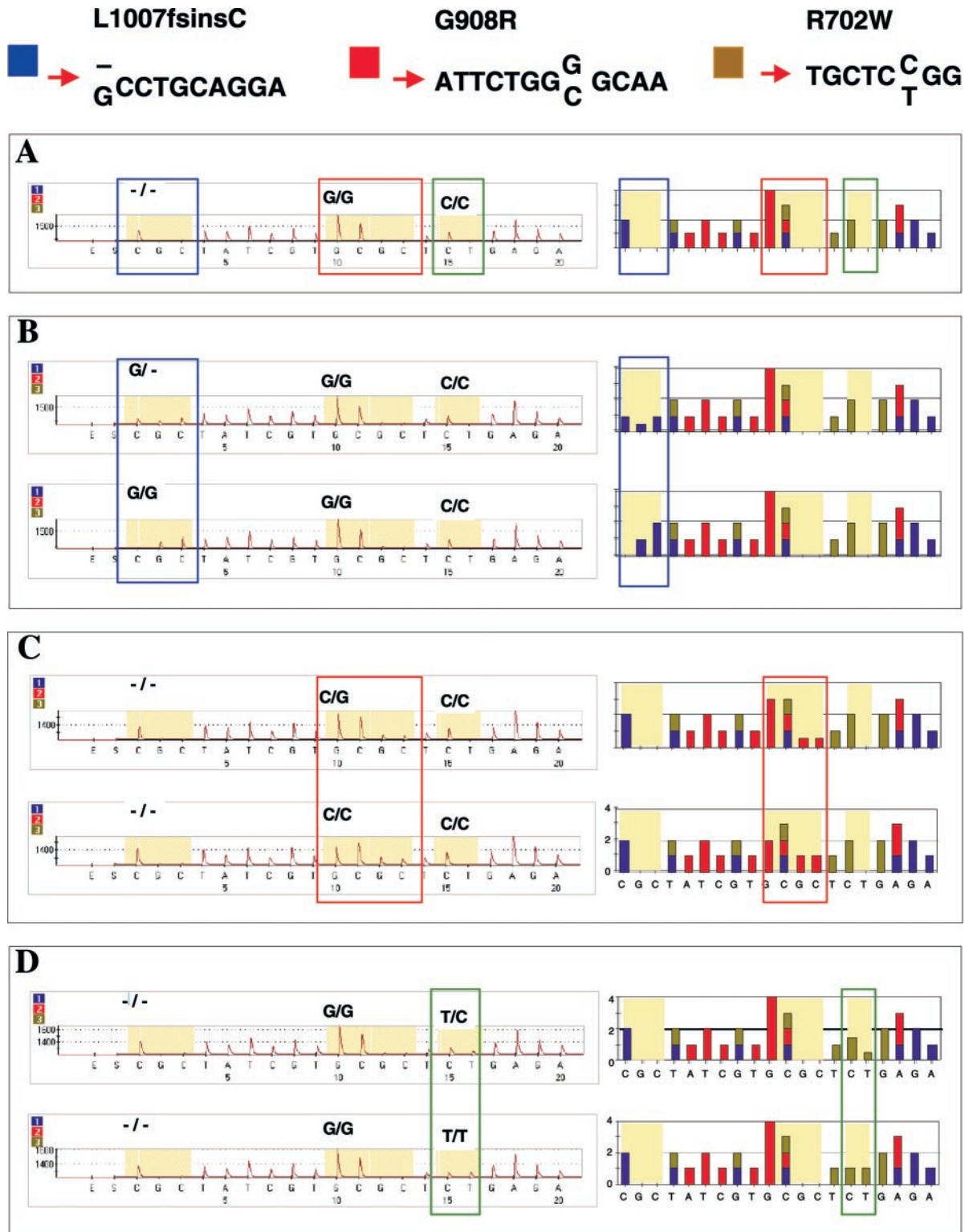
Fig. 1. Simultaneous pyrosequencing results for L1007fsinsC (insertion C), G908R (G to C), and R702W (C to T) in *CARD15* gene.

The three SNPs to be interrogated simultaneously are color-coded and depicted at the *top* with the expected read-outs from the three different combined Pyrosequencing sequencing primers (*red arrows*), each of which stops one base short of the three sequences shown. Homozygous wild-type individuals are shown in *panel A* with the experimental and theoretical pyrograms on the *left* and *right*, respectively. The reaction contains all three primers, and the theoretical sequence contribution of each color-coded allele at each position is indicated by the *colored columns* in the pyrograms on the *right* (e.g., in *panel A*, C extension in the *red box* for G908R contains nucleotide contributions from each of the three alleles). Details of the contribution of each SNP to the theoretical pyrograms are described in the text. Experimental and theoretical pyrograms for heterozygous (*top*) and homozygous mutant (*bottom*) genotypes for SNP L1007fsinsC, G908R, and R702W are shown in *panels B, C,* and *D* on the *left* and *right*, respectively.

as individual peaks in the pyrogram. Pyrograms (left) and the theoretical Pyrosequencing results (right) for the three wild-type regions and six different genotypes are shown in panels A and B–D of Fig. 1, respectively. The contribution to the theoretical sequence readout at each nucleotide position by each of three different SNP regions is indicated in different colors on the right (blue for L1007fsinsC, red for G908R, and brown for R702W). Incorporation of each nucleotide for each allele produces a 0.5 peak height.

The blue boxes in panels A and B show results for the L1007fsinsC SNP extension reaction. L1007fsinsC is produced by a one-base insertion at nucleotide 3020 in exon 11 of the gene, which causes a frameshift mutation (20, 21). The wild-type genotype pyrogram for the L1007fsinsC is shown in Fig. 1A, with the nucleotide dispensation order indicated above; the primer extension produces a double C peak height (e.g., 0.5×4 Cs; 2 for each wild-type allele) followed by no signals for G or C at the next two positions. The results for a heterozygote for G insertion at SNP L1007fsinsC are shown in the top portion of Fig. 1B, with the primer extension producing a single C peak (0.5×2 Cs from the wild-type allele), a half-magnitude G peak (0.5×1 G from the variant SNP), and a single C peak (0.5×2 Cs from the variant SNP). The results for homozygosity for the G insertion are shown in the bottom portion of Fig. 1B, with the primer extension producing no C peak, followed by a single G peak (corresponding to 0.5×2 Gs for the G insertion in both alleles) and a double C peak (0.5×4 Cs; 2 from each insertion G allele).

The red boxes in panels A and C of Fig. 1 show results for the G908R SNP extension reaction. G908R is caused by a G-to-C base substitution at nucleotide 2722 in exon 8 of the gene, producing a missense mutation (20, 21). Results for the wild-type genotype are shown in Fig. 1A, with a quadruplicate G peak (0.5×4 Gs in each allele) and a triple C peak (0.5×2 Cs from the two wild-type alleles at this locus plus 0.5×2 Cs each from the two wild-type alleles at the L1007fsinsC and R702W loci), followed by no G and no C peaks (indicating no mutation). The bottom portion of Fig. 1C shows the results for homozygosity for the G908R SNP, which produces a double G peak followed by a triple C (as indicated above), a single G, and a single C peak. The top portion in Fig. 1C shows the results for heterozygosity at G908R with a triple G (0.5×4 Gs from the wild-type allele and 0.5×2 Gs from the variant) and C peaks (as indicated above), and half G and C peaks attributable to the mutation.

The peaks in the green boxes are results for extension reactions for wild-type, heterozygous, and mutant/mutant genotypes for R702W, a C-to-T base substitution at nucleotide 2104 in exon 4 of the gene, which produces a missense mutation (20, 21). Results are completely concordant with the theoretical expectation (Fig. 1, A and D).

Allele and genotype frequencies were calculated from the families' probands, and differences between patients and controls were tested by the Fisher exact and χ^2 tests, respectively. The frequency of L1007fsinsC was significantly higher in probands from the CD and mixed families than in controls, but not in probands from the UC families ($P = 0.0002$, 0.00002, and 0.38, respectively). In addition, the frequency of G908R was significantly higher in probands of CD families ($P = 0.01$). These frequencies are similar to those observed in other European populations (7). From the same data, we calculated that the relative risk of CD was 4.05 (95% confidence interval, 1.92–8.53) for heterozygotes and homozygotes for any of the CARD15 SNP variants (Table 1). No Mendelian inheritance error was found. All 365 samples were scored correctly compared to automated DNA sequence analyses. Our experience demonstrates several advantages of Pyrosequencing (23–25), including a relatively easy and low-cost set up and a multiplexing capability that facilitates simultaneous detection of DNA variations that map to different sites in the same template. The use of nonproprietary supplies from the hardware manufacturers decreases the cost of Pyrosequencing, and template preparation can be standardized and robotically automated, allowing 96 samples to be sequenced in 25 min.

Table 1. Genotype and allele frequency distributions in probands and controls based on SNP distribution.

SNP	Group	Genotype frequency, n −/−	+/−	+/+	Allele frequency, %	P^a
R702W	CD	37	10		0.11	0.10
	UC	46	3		0.03	0.41
	Mixed	15	3		0.08	0.71
	Controls	96	11	1	0.06	
G908R	CD	39	8		0.09	0.01
	UC	46	3		0.03	0.71
	Mixed	17	1		0.03	1.00
	Controls	103	5		0.02	
L1007fsinsC	CD	39	7	1	0.10	0.0002
	UC	46	3		0.03	0.38
	Mixed	13	4	1	0.17	0.00002
	Controls	105	3		0.01	

^{a} P for difference in allele frequencies between probands and controls (Fisher exact test).

References

1. Sandler RS. Epidemiology of inflammatory bowel disease. In: Targan SR, Shanahan F, eds. Inflammatory bowel disease. From bench to bedside. Baltimore: Williams & Wilkins, 1994:5–31.
2. Satsangi J, Jewell DP, Bell JI. The genetics of inflammatory bowel disease. Gut 1997;40:572–4.
3. Ahmad T, Armuzzi A, Bunce M, Mulcahy-Hawes K, Marshall SE, Orchard TR, et al. The molecular classification of the clinical manifestations of Crohn's disease. Gastroenterology 2002;122:854–66.
4. Farrell RJ, Peppercorn MA. Ulcerative colitis. Lancet 2002;359:331–40.
5. Shanahan F. Crohn's disease. Lancet 2002;359:62–9.
6. Cuthbert AP, Fisher SA, Mirza MM, King K, Hampe J, Croucher PJ, et al. The contribution of NOD2 gene mutations to the risk and site of disease in inflammatory bowel disease. Gastroenterology 2002;122:867–74.
7. Lesage S, Zouali H, Cezard JP, Colombel JF, Belaiche J, Almer S, et al. CARD15/NOD2 mutational analysis and genotype-phenotype correlation in 612 patients with inflammatory bowel disease. Am J Hum Genet 2002;70:845–57.
8. Hampe J, Grebe J, Nikolaus S, Solberg C, Croucher PJP, Mascheretti S, et al. Association of NOD2 (CARD15) genotype with clinical course of Crohn's disease: a cohort study. Lancet 2002;359:1661–5.
9. Vermeire S, Wild G, Kocher K, Cousineau J, Dufresne L, Bitton A, et al. CARD15 genetic variation in a Quebec population: prevalence, genotype-phenotype relationship, and haplotype structure. Am J Hum Genet 2002;71:74–83.
10. Bonen DK, Cho JH. The genetics of inflammatory bowel disease [Review]. Gastroenterology 2003;124:521–36.
11. Hugot JP, Laurent-Puig P, Gower-Rousseau C, Olson JM, Lee JC, Beaugerie L, et al. Mapping of a susceptibility locus for Crohn's disease on chromosome 16. Nature 1996;379:821–3.
12. Mirza MM, Lee J, Teare D, Hugot JP, Laurent-Puig P, Colombel JF, et al. Evidence of linkage of the inflammatory bowel disease susceptibility locus on chromosome 16 (IBD1) to ulcerative colitis. J Med Genet 1998;35:218–21.
13. Duerr RH, Barmada MM, Zhang L, Davis S, Preston RA, Chensny LJ, et al. Linkage and association between inflammatory bowel disease and a locus on chromosome 12. Am J Hum Genet 1998;63:95–100.
14. Cho JH, Nicolae DL, Gold LH, Fields CT, LaBuda MC, Rohal PM, et al. Identification of novel susceptibility loci for inflammatory bowel disease on chromosomes 1p, 3q, and 4q: evidence for epistasis between 1p and IBD1. Proc Natl Acad Sci U S A 1998 23;95:7502–7.
15. Annese V, Latiano A, Bovio P, Forabosco P, Piepoli A, Lombardi G, et al. Genetic analysis in Italian families with inflammatory bowel disease supports linkage to the IBD1 locus. A GISC study. Eur J Hum Genet 1999;7:567–73.
16. Forabosco P, Collins A, Latiano A, Annese V, Clementi M, Andriulli A, et al. Combined segregation and linkage analysis of inflammatory bowel disease in the IBD1 region using severity to characterise Crohn's disease and ulcerative colitis. Eur J Hum Genet 2000;8:846–52.
17. Cavanaugh J, IBD International Genetics Consortium. International collaboration provides convincing linkage replication in complex disease through analysis of a large pooled data set: Crohn disease and chromosome 16. Am J Hum Genet 2001;68:1165–71.
18. van Heel DA, McGovern DP, Cardon LR, Dechairo BM, Lench NJ, Carey AH, et al. Fine mapping of the IBD1 locus did not identify Crohn disease-associated NOD2 variants: implications for complex disease genetics. Am J Med Genet 2002;111:253–9.
19. Ronaghi M. Pyrosequencing sheds light on DNA sequencing [Review]. Genome Res 2001;11:3–11.
20. Hugot JP, Chamaillard M, Zouali H, Lesage S, Cezard JP, Belaiche J, et al. Association of NOD2 leucine-rich repeat variants with susceptibility to Crohn's disease. Nature 2001;411:599–603.
21. Ogura Y, Bonen DK, Inohara N, Nicolae DL, Chen FF, Ramos R, et al. A frameshift mutation in NOD2 associated with susceptibility to Crohn's disease. Nature 2001;411:603–6.
22. Hampe J, Cuthbert A, Croucher PJ, Mirza MM, Mascheretti S, Fisher S, et al. Association between insertion mutation in NOD2 gene and Crohn's disease in German and British populations. Lancet 2001;357:1925–8.
23. Fakhrai-Rad H, Pourmand N, Ronaghi M. Pyrosequencing: an accurate detection platform for single nucleotide polymorphisms [Review]. Hum Mutat 2002;19:479–85.
24. Ferraris A, Rappaport E, Santacroce R, Pollak E, Krantz I, Toth S, et al. Pyrosequencing for detection of mutations in the connexin 26 (GJB2) and mitochondrial 12S RNA (MTRNR1) genes associated with hereditary hearing loss. Hum Mutat 2002;20:312–20.
25. Nordfors L, Jansson M, Sandberg G, Lavebratt C, Sengul S, Schalling M, et al. Large-scale genotyping of single nucleotide polymorphisms by pyrosequencing and validation against the 5' nuclease (Taqman) assay. Hum Mutat 2002;19:395–401.

Single-Tube Multiplex-PCR Screen for Anti-3.7 and Anti-4.2 α-Globin Gene Triplications

Wen Wang,[1] Edmond S.K. Ma,[5] Amy Y.Y. Chan,[5] John Prior,[7] Wendy N. Erber,[7] Li C. Chan,[5] David H.K. Chui,[6] and Samuel S. Chong[1–4]* (Departments of [1] Pediatrics and [2] Obstetrics & Gynecology, National University of Singapore, Singapore 119074, Singapore; [3] The Children's Medical Institute and Molecular Diagnosis Center, Department of Laboratory Medicine, National University Hospital, Singapore 119074, Singapore; [4] Departments of Pediatrics and Gynecology & Obstetrics, The Johns Hopkins University School of Medicine, Baltimore, MD 21287; [5] Division of Hematology, Department of Pathology, The University of Hong Kong and Queen Mary Hospital, Hong Kong, People's Republic of China; [6] Departments of Medicine and Pathology, Boston University School of Medicine, Boston, MA 02118; [7] The Western Australian Centre for Pathology and Medical Research, Nedlands, WA 6009, Australia; * address correspondence to this author at: Department of Pediatrics, National University of Singapore, Level 4, National University Hospital, 5 Lower Kent Ridge Road, Singapore 119074, Singapore; fax 65-6779-7486, e-mail paecs@nus.edu.sg)

The coexistence of α-globin gene triplication (ααα) is an important modulator of the severity of β-thalassemia trait or β-thalassemia intermedia, exacerbating the phenotypic severity of β-thalassemia by causing more globin chain imbalance *(1, 2)*. Typically, the inheritance of a single β-thalassemia allele is associated with mild anemia and hypochromic microcytic red cells. Compared with simple β-heterozygotes, co-inheritance of triplicated or quadruplicated α-globin genes in β-heterozygotes often leads to more significant anemia, splenomegaly, more pronounced red cell abnormalities, the presence of circulating normoblasts, higher hemoglobin F concentrations, and even the presence of inclusion bodies in erythroblasts *(3, 4)*. Because the α- and β-globin gene clusters are physically unlinked and segregate independently,